Vol. 21: 59–81, 2002 | CLIMATE RESEARCH Clim Res | Published May 23

Persistence and periodicity in the precipitation series of Turkey and associations with 500 hPa geopotential heights

M. Türkeş*, U. M. Sümer, G. Kılıç

State Meteorological Service, Department of Research, PO Box 401, Ankara, Turkey

ABSTRACT: Persistence and periodicity in normalised precipitation anomaly series of 91 stations over Turkey were analysed using serial correlation coefficients and power spectra. There were considerable geographical variations and inter-seasonal contrasts with respect to periodicity and persistence characteristics. Lag-one serial correlation (*L*-1*SC*) coefficients for winter series were mostly positive and were significant at the 0.05 level for 31 stations. Annual variations at 17 stations also showed significant positive *L*-1*SC* coefficients. In contrast, year-to-year variations in spring series were characterised by negative *L*-1*SC* coefficients at most stations (significant at 18). Summer series were characterised by both positive and negative coefficients. Autumn series of most stations were random with regard to serial dependence. For winter series, long cycles of 8.4, 12–12.7, 14, 18 and 21 yr were dominant in the Marmara Transition and the Mediterranean regions, whereas short cycles of 2, 2.1, 3 and 3.2 yr were found for the Black Sea region. Major spectral peaks of most spring series occurred within spectral bands with cycles of around 2, 3, 4 and 5 yr; a 2 yr periodicity was obtained for many stations. Statistically significant negative relationships between precipitation anomalies and 500 hPa geopotential height anomalies in winter and autumn showed an apparent spatial coherence over most of Turkey. Prominent spectral peaks corresponding to about 2 and 3 yr cycles in spring precipitation anomaly series appeared to be associated with similar oscillations in spring geopotential height anomalies. A cycle of 14 yr was found for winter precipitation and geopotential height anomalies.

KEY WORDS: Turkey · Precipitation · 500 hPa geopotential height · Persistence · Power spectrum · 'White' and 'red' noise continuum · Periodicity

1. INTRODUCTION

To understand natural and human-induced climatic change or global warming and to mitigate its impacts and develop policies, we monitor and model the climate system. Long-term systematic observations are of vital importance in order to understand natural variability of climate, determine human impacts on the climate system, parameterise the main processes required in models and verify model simulations. One of the ways to examine natural variability and changes in the climate system as well as all the ecological responses to them is time-series analysis of paleoclimatic and historical data and instrumental climatological (and climate-related hydrological and atmospheric) observation records.

Most climate models produce estimates of decreasing or increasing trends in means of the climatological elements for the future climate changes. However, in addition, climate models should represent all the deterministic components of the climatological time-series, such as serial dependence (persistence) and periodicity. This requires an understanding of the present statistical and climatological characteristics of persistence and periodic components of a long-term time-series.

*E-mail: mturkes@meteor.gov.tr

Time-series characteristics of climatological and hydrological observation records can be assigned to the following categories for examination: (1) A stochastic event including random variations or stable processes. (2) Deterministic components corresponding to all the non-random events in the series. Deterministic components include persistence, periodicity, trends, jumps or step-wise changes, catastrophic events (for example, disasters or extreme events), and various combinations of these. (3) A combination of random and non-random events in the series. The third category is important for long-term temporal variations in a series of climatic observations. Based on both real observational records and statistical models, it is well known that trends in climatological series are rarely linear and cycles are rarely purely sinusoidal waves. This peculiarity is found particularly in temporal variations of precipitation series. For instance, a significant downward trend has been revealed for the winter precipitation series at some stations in Turkey (Türkeş 1998). Nevertheless, this trend is not linear. In fact, the series exhibit a low-frequency fluctuation around a decreasing mean.

Understanding the relationships between climatic (here, precipitation) variations and various physical (here, atmospheric) mechanisms is not only important for present changes but also for future changes in the climate system.

A preliminary study of the variations in 700 hPa (and in some cases 500 hPa) geopotential heights over Turkey indicated that the low-frequency fluctuations in winter and the high-frequency oscillations in spring were dominant in the upper atmospheric conditions (Türkeş 1998). These variation types were reflected in the spatial and temporal precipitation variations over much of Turkey. According to a very recent study (Kutiel et al. 2001), the relationship between regional sea-level pressure (SLP) patterns and dry or wet monthly precipitation conditions over Turkey is significant in winter and non-existent in summer. Pressure patterns associated with dry conditions usually show positive SLP departures, and vice versa. There is a strong relationship between pressure patterns associated with wet conditions and correlation maps for the same months. Similar atmospheric variations and relationships have been found for precipitation over the eastern Mediterranean Basin and Greece, especially during winter (Maheras et al. 1999, Xoplaki et al. 2000). Xoplaki et al. (2000) investigated the influence of the large-scale winter mid-tropospheric circulation on Greek precipitation anomalies by means of empirical orthogonal functions and canonical correlation analysis. They concluded that the spatial distribution of winter precipitation over Greece was related to the eastern North Atlantic-European mid-tropospheric circulation fields. Mächel et al. (1998) revealed for time-series with the 'white' noise continuum that significant peaks above the 0.95 confidence limit occurred only at the lowest frequency in both the central pressure spectra of the subtropical highs in winter and the spectra of the latitudinal and longitudinal position of the Iceland Low in summer. The spectra of time-series compared with the 'red' noise continuum also showed that most of the total variance accumulated at the lowest frequency. This was detected for the spectrum of the latitudinal location of the Inter Tropical Convergence Zone in winter and for the spectra of the latitudinal and longitudinal positions of the Azores High central pressure. Türkeş (1998) suggested for Turkey that quasi-biennial oscillations in both spring precipitation and geopotential heights and 14 and 13 yr periodicity in annual or winter precipitation and geopotential heights, respectively, may have been linked with the quasi-biennial and 13.2 yr cyclicities in the monthly zonal index series of surface pressure for the 35 to 65° N zone, which were reported by Kozuchowski (1993). Kozuchowski also indicated that the quasi-biennial and 13 yr cyclicities appeared in seasonal values of the zonal index.

In the present study, persistence (serial dependence) and periodicity from components of non-randomness in long-term annual and seasonal precipitation series of 91 stations over Turkey were investigated with respect to climatic variability. Some effects of variations in the 500 hPa geopotential height series at the İstanbul station (Göztepe) on variations in the precipitation series over Turkey were also examined. The 500 hPa height data were analysed in order to show relationships between the variations and periodicity of the upper atmospheric level height series and those of the precipitation series.

2. DATA

The precipitation data set that was developed originally by Türkeş (1995, 1996) was used in this study. It consists of monthly precipitation totals (mm) recorded at the 91 stations of the Turkish State Meteorological Service (TSMS) during the period 1930–1996. These stations were selected from about 130 climatology and precipitation stations by Türkeş (1995, 1996), after possible inhomogeneity types, particularly those of step-wise changes (non-climatic abrupt changes) in monthly and seasonal precipitation series, were detected by applying the Kruskall-Wallis homogeneity tests. Results of the homogeneity tests were also controlled by means of graphical time-series analyses and with the station history information file collected for the stations. Procedures for the estimation of missing

values in precipitation series and for the homogeneity analysis were given in detail by Türkeş (1995, 1996).

At this point, we recognize that it would be useful to give the necessary information about the frequency distribution and secular trend characteristics for the long-term annual and seasonal precipitation series of Turkey. Most of the annual precipitation total series show positive skewness to some degree (Türkeş 1995, 1996). Nevertheless, the frequency distribution for some stations fits a normal, except for summer. The frequency distribution approaches a theoretically normal distribution as the record length increases. For the stations used in the present study, Türkeş (1996, 1998) found significant decreasing or increasing secular trends in some precipitation series. Normalised annual and winter precipitation anomaly series decreased significantly at 15 and 14 stations, respectively, most of which are located in the Mediterranean rainfall region. Spring, summer and autumn precipitation series are mostly random versus the significant secular trends. Long-term variations in precipitation series, however, were generally characterised by successive periods of wetter and drier than normal precipitation conditions. For annual and winter precipitation anomaly series, wet conditions generally occurred during the 1940s, 1960s, late 1970s, early 1980s and mid-to-late 1990s, whereas dry conditions generally dominated in the early-to-mid 1930s, early-to-mid 1970s, mid-to-late 1980s, early 1990s, and 1999/2000 over most of Turkey (Türkeş 1998, 2002). Spring precipitation series generally indicated an upward trend from the mid 1940s to the late 1960s at many stations and to 1980s at some stations. This period was generally followed by a downward trend at many stations. Summer rainfall series tended to increase significantly at 7 stations.

The geographical distribution of the 91 stations with regard to the rainfall regime regions of Turkey is shown in Fig. 1 and the fundamental characteristics of the rainfall regions are given in Table 1. The rainfall regime regions of Turkey were originally designated by Türkeş (1996).

In addition to precipitation data, we have made use of 500 hPa geopotential height level (standard upper atmospheric level) observations, which were recorded at the İstanbul (Göztepe) radiosonde station. The upper air data covers the period 1952–1993. Due to the geographical position of İstanbul in the Marmara region of Turkey, variations of 500 hPa geopotential heights at the İstanbul radiosonde station are a likely indicator (or a representative) of variations of the dynamic atmospheric pressure systems that originate in both the North Atlantic and the Mediterranean (i.e. lows and troughs; highs and ridges). A more comprehensive analysis of the variations and trends in the 700 hPa (and in some cases 500 hPa) geopotential height series was made by Türkeş (1998).

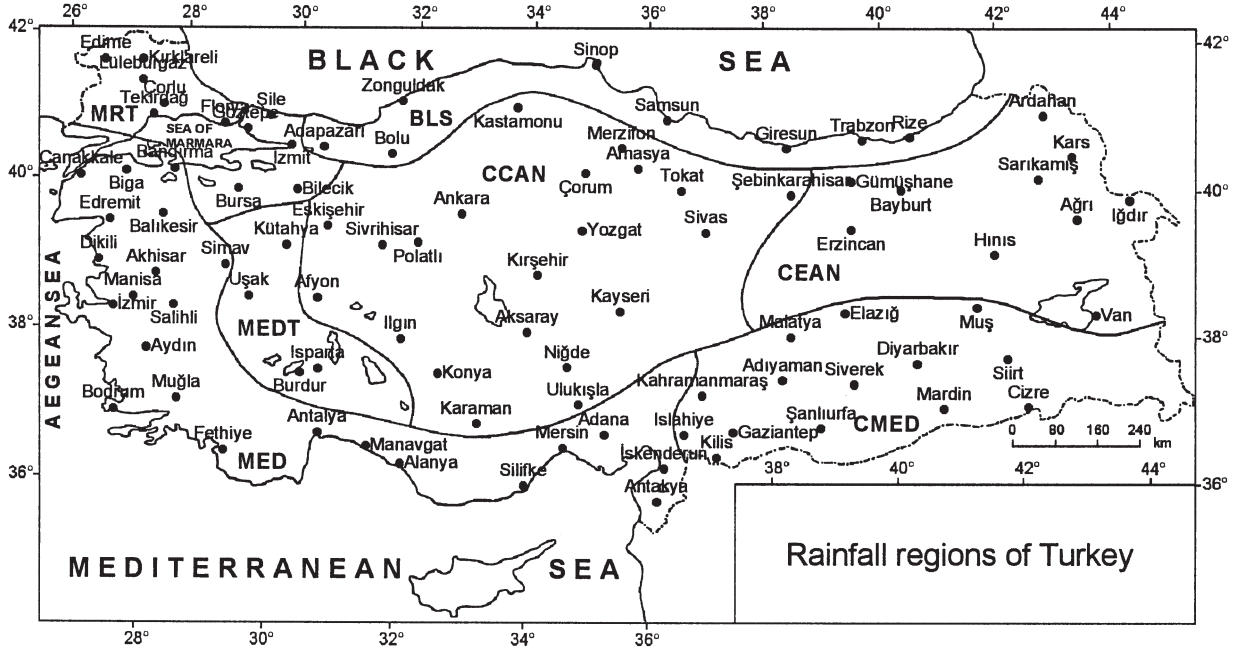

Fig. 1. Geographical distribution of Turkey's rainfall regime regions and the 91 stations used in this study. BLS: Black Sea; MRT: Marmara Transition; MED: Mediterranean; CMED: Continental Mediterranean; MEDT: Mediterranean Transition; CCAN: Continental Central Anatolia; CEAN: Continental Eastern Anatolia. Re-plotted from Türkeş (1998)

Table 1. Basic characteristics of the rainfall regime regions of Turkey (Türkeş 1996)

Rainfall region	Number of stations
Black Sea (BLS): Uniformly rainy with a maximum in autumn; temperate	8
Marmara Transition—Mediterranean to Black Sea—(MRT): Quite uniformly rainy with a warm and light rainy summer	11
Mediterranean (MED): Markedly seasonal with a cool and heavily rainy winter and a hot dry summer; humid and semi-humid subtropical	23
Continental Mediterranean (CMED): Seasonal with a rainy winter and spring and a severe hot dry summer; semi-arid and dry semi-humid subtropical	14
Mediterranean Transition—Mediterranean to Central Anatolia—(MEDT): Moderately rainy winter and spring	4
Continental Central Anatolia (CCAN): Cool rainy spring, cold rainy winter, and warm and light rainy summer; semi-arid and dry semi-humid steppe	21
Continental Eastern Anatolia (CEAN): Cool rainy spring and early summer with a very cold and snowy winter; dry semi-humid and semi-humid steppe and highland	10

3. METHOD OF ANALYSIS

Normalised precipitation and geopotential height anomaly series were used. A normalised precipitation (or geopotential height) anomaly (A_{sy}) for a long series of a given station is

$$A_{sy} = (P_{sy} - \overline{P}_s)\big/\sigma_s$$

where P_{sy} is total precipitation amount (mm) for station s during year y (or season); $\overline{P}_s$ and σ_s are the long-term average and standard deviation of annual (or seasonal) precipitation series for that station, respectively.

3.1. Computation of the power spectrum

Periodicity is one of the non-random types (deterministic events) in time-series. Most of the climatic, atmospheric and hydrological time-series would consist of a combination of stochastic and deterministic components. The power spectrum is a method of analysis that was developed to handle the problem of periodicity in variations of natural events observed in time, such as in climatological and hydrological time-series. Power spectrum analysis, also called generalised harmonic analysis, was derived from the principles first developed by Wiener (1930, 1949).

Even though procedures for computing the power spectra vary, we have followed an approach, as described in WMO (1966), developed by Tukey (1950) and Blackman & Tukey (1958). A detailed description of this approach can also be found in various textbooks: Blackman & Tukey (1958), Jenkins & Watts (1968) and Julian (1967). It can be summarised as follows:

First, serial correlation (or autocorrelation) coefficients of normalised climatic series are computed for all lags from $L = 0$ to m, where m is the maximum lag equal to about $\frac{1}{3}$ of the length of series N, by using the following formula:

$$r_L = \frac{(N-L)\sum_{i=L}^{N-L} x_i x_{i+L} - \left(\sum_{i=L}^{N-L} x_i\right)\left(\sum_{i=L+1}^{N} x_i\right)}{\left[(N-L)\sum_{i=L}^{N-L} x_i^2 - \left(\sum_{i=L}^{N-L} x_i\right)^2\right]^{1/2}\left[(N-L)\sum_{i=L+1}^{N} x_i^2 - \left(\sum_{i=L+1}^{N} x_i\right)^2\right]^{1/2}} \quad (1)$$

Then, 'raw' spectral estimates, s_k, are found directly from these r_L values by using the following equations:

(a) For the zeroth spectral estimate,

$$\hat{s}_0 = \frac{1}{2m}(r_0 + r_m) + \frac{1}{m}\sum_{L=1}^{m-1} r_L$$

(b) For all the intervening $m - 1$ spectral estimates, $k = 1, 2, \ldots, m-1$,

$$\hat{s}_k = \frac{r_0}{m} + \frac{2}{m}\sum_{L=1}^{m-1} r_L \cos\left(\frac{\pi k L}{m}\right) + \frac{1}{m} r_m (-1)^k \quad (2)$$

(c) For the last spectral estimate, which is the shortest wavelength in the spectrum (here 2 yr),

$$\hat{s}_m = \frac{1}{2m}[r_0 + (-1)^m r_m] + \frac{1}{m}\sum_{L=1}^{m-1}(-1)^L r_L$$

Finally, final spectral estimates s_k are computed by smoothing the 'raw' estimates with a 3-term weighted average. In the smoothing procedure, smoothing equations of the Hanning method are used (WMO 1966):

$$\text{(a)} \quad s_0 = \frac{1}{2}(\hat{s}_0 + \hat{s}_1)$$

$$\text{(b)} \quad s_k = \frac{1}{4}(\hat{s}_{k-1} + 2\hat{s}_k + \hat{s}_{k+1}) \quad (3)$$

$$\text{(c)} \quad s_m = \frac{1}{2}(\hat{s}_{m-1} + \hat{s}_m)$$

The averaging procedure is performed to derive a consistent estimate of the final spectrum in terms of $m + 1$ discrete estimates (WMO 1966).

3.2. Tests of statistical significance for the power spectra

A set procedure for the tests of statistical significance, which was proposed by WMO (1966) to be applied to power spectra of climatic series, is used for an objective assessment of the spectral estimates from the power spectrum analysis. The theory and application of this procedure are given below:

First, a 'null' hypothesis continuum is fitted to the computed spectrum. To start this step, significance of the Lag 1 serial correlation (L-1SC) coefficient, r_1, of the climatic series is tested by the following formula of the hypothesis test:

$$(r_1)_t = \frac{-1 \pm t_g \sqrt{N-1}}{N-1} \quad (4)$$

where t_g is 1.645 for the 0.05 level of significance, according to the 1-sided test of normal distribution. The null hypothesis of randomness of climatic series against the serial correlation is rejected for the large values of $(r_1)_t$.

If the L-1SC coefficient, r_1, of a series of observations is not statistically significant, or is significant but has a negative sign, it is assumed that the series does not contain persistence. In this case, the appropriate null continuum is white noise. In other words, a horizontal straight line, the value of which is everywhere equal to the average of the values of all $m + 1$ 'raw' spectral estimates in the computed spectrum, is taken as the most suitable theoretical approach. On the other hand, if the computed r_1 is positive and statistically significant, serial correlation coefficients for Lag 2 and Lag 3 are checked to see whether they approximate the exponential relations $r_2 \cong r_1^2$ and $r_3 \cong r_1^3$ (WMO 1966). If these relations are ensured with the computed serial coefficients, the appropriate null continuum is assumed as the simple Markov red noise, whose shape depends on unknown value of the L-1SC coefficient for a population, P.

Then, the continuum can be created by following approximate procedure. By assuming that the sample r_1 is an unbiased estimation of P, various choices of the harmonic number of k between $k = 0$ and m are assessed:

$$S_k = \bar{s}\left(\frac{1-r_1^2}{1+r_1^2-2r_1\cos\left(\frac{\pi k}{m}\right)}\right) \quad (5)$$

where $\bar{s}$ is the average of all $m + 1$ 'raw' spectral estimates, $\hat{s}_k$, in the computed spectrum. The resulting values of S_k can be plotted superposed on the sample spectrum, and a smoothed curve passed through these values to reach the required null continuum.

Finally, if it is found that r_1 is statistically significant but a few serial correlation coefficients for higher lags do not show the required exponential relations with r_1, then doubt arises as to whether the simple Markov-type persistence is the dominant form of non-randomness in series of climatic observations. In this circumstance, the Markov red noise continuum may not be appropriate. Nevertheless, WMO (1966) suggested that this procedure could be continued with just as before to compute the red noise continuum for r_1.

At this stage of the power spectrum analysis, a first choice of the null continuum is made, and this selected continuum is superposed on the studied spectrum. In this case, it would be possible to make an assessment of the spectrum for its consistency with the chosen continuum. Then, the value of each spectral estimate s_k is compared with the local value of the null continuum.

The statistic associated with the each spectral estimate is the ratio of the magnitude of the spectral estimate to the local magnitude of the continuum (red noise continuum). Tukey (1950) found that the quantity of this ratio is distributed as chi-square divided by the degrees of freedom. The degrees of freedom, ν, of each estimate of a computed spectrum is given by

$$\nu = \frac{2N - m/2}{m} \quad (6)$$

where N is the length of series and m is the maximum lag.

The ratio of any sample spectral estimate s_k to its local value of the red noise continuum is then compared with critical percentage-point levels of a χ^2/ν distribution for the proper ν value. This comparison produces the required statistical significance level. The χ^2 values can be obtained from a statistic reference book. In a sample spectrum, critical percentage-point levels of the χ^2/ν distribution, e.g. the 0.95 confidence limit, is the same for all spectral estimates s_k.

4. RESULTS OF THE ANALYSIS

4.1. Persistence

The definition of persistence by WMO (1966), which is very common for the studies of climatic variability and change, has been taken as a basis. According to this definition, persistence is 'a tendency for successive values of the series to "remember" their antecedent values, and to be influenced by them.' The L-1SC coefficient r_1 has been used to detect possible persistence in observed year-to-year variations of

normalised precipitation anomaly series and to examine its nature and magnitude. The approach proposed by WMO (1966) and Matalas (1967) was widely used later in many studies related to long-term climatic variations (e.g. Rodhe & Virji 1976, Granger 1977, Ogallo 1979, Anyadike 1993, Drosdowsky 1993, Nicholson & Palao 1993, Türkeş 1998, 1999). Persistence is evident in long series of climatic observations characterised by a positive serial correlation. Significant negative *L*-1*SC* coefficients are very likely to be indicative of high-frequency oscillations, whereas significant positive *L*-1*SC* coefficients are likely to be indicative of low-frequency fluctuations and persistence in climatic series.

In this study, serial correlation (autocorrelation) coefficients were computed for all lags from $L = 0$ to m, where m is equal to about one-third of the number of observations. We have used and assessed the serial correlation coefficients of the first 3 lags for this subsection, and the series of serial correlation coefficients computed for all lags to m have been taken into account in Section 4.2.

Field analysis was performed to reveal the geographical distribution patterns of the Lag 1, Lag 2 and Lag 3 autocorrelation coefficients over Turkey. The field analysis transforms data of irregularly distributed stations in space into a regular grid system. An interpolation method was used in order to produce contours of spatial distribution maps. This method has been applied to the stations' data by means of a mapping package. The gridding method of kriging with a linear variogram model was chosen for this purpose. This model is very successful for the original climatic variables and their resultant statistics, particularly for precipitation data, and generates a better overall interpretation of the spatial distribution patterns and coherent regions. Detailed descriptions of the kriging approach can be found in many publications, such as Delfiner & Delhomme (1975), Cressie (1991) and Bardossy & Muster (1993). Although all maps were prepared for the study, only the maps belonging to serial correlation coefficients of the annual, winter and spring precipitation series are given here. This is due to the fact that summer and autumn precipitation series of most stations were found to be statistically random versus the serial correlation and do not show a clear spatial coherence over Turkey.

Normalised winter precipitation series indicate persistence at many stations, except those in the Black Sea rainfall region (Fig. 2a). This is indicated by the positive Lag 1 serial correlation (*L*-1*SC*) coefficients. Persistence of winter precipitation series from year-to-year variations was statistically significant at the 0.05 significance level for 31 stations. Detailed tables were prepared for the annual and seasonal results of the 91 stations but are not given here. The geographical distribution pattern of winter precipitation does not show an apparent spatial coherence for the stations that are characterised by the statistically significant positive *L*-1*SC* coefficients (Fig. 2a). Some coherent areas with significant positive serial correlations exist over the western and eastern regions of Turkey. Many annual precipitation series are also characterised by positive *L*-1*SC* coefficients (Fig. 2b). The *L*-1*SC* coefficients for annual precipitation series are significant at the 0.05 level for 17 stations. Spatial coherence of the significant *L*-1*SC* coefficients for annual precipitation is similar to that for the winter pattern in Fig. 2a. This similarity can be attributed to the fact that the percentage contribution of winter precipitation to the annual total is quite large (Türkeş 1998). This is particularly pronounced for the stations located over the MED rainfall regime region. The positive *L*-1*SC* coefficients for the winter precipitation series are generally greater than those of the annual series, with the exception of those over the western and northwestern parts (Antalya subregion) of the MED region. In spring season, however, year-to-year precipitation variations of most stations are characterised by negative *L*-1*SC* coefficients. Negative *L*-1*SC* coefficients for the spring series are statistically significant at 18 stations. These stations are mostly distributed over the CCAN, CEAN and CMED rainfall regions (Fig. 2c). There is only 1 large area of coherence with significant negative *L*-1*SC* coefficients over the CMED region, even though the distribution pattern exhibits several areas throughout the country which are characterised by significant negative *L*-1*SC* coefficents (Fig. 2c). It is seen that year-to-year variations in summer rainfall series of some stations are described by negative *L*-1*SC* coefficients, whereas some of summer precipitation series are associated with positive *L*-1*SC* coefficients, 9 of which are statistically significant. Autumn precipitation series have both positive and negative *L*-1*SC* coefficients, and all series except those of 4 stations are random with regard to the serial correlation. In other words, interannual variations of summer and autumn precipitation series can be considered to be distributed independent of time.

The Lag 2 serial correlation (*L*-2*SC*) coefficients of winter precipitation series (Fig. 3a) are generally positive at many stations, but they are smaller than the *L*-1*SC* coefficients in Fig. 2a. Some values discordant (maximum and minimum) with their surroundings are observed over the western coast and northeastern part of the MED region, respectively. There is also an area of insignificant negative *L*-2*SC* coefficients over the central and central northeastern parts (Fig. 3a). The *L*-2*SC* coefficients for the annual precipitation series are mostly positive but insignificant. Distribution pattern of the *L*-2*SC* coefficients in Fig. 3b seems to be

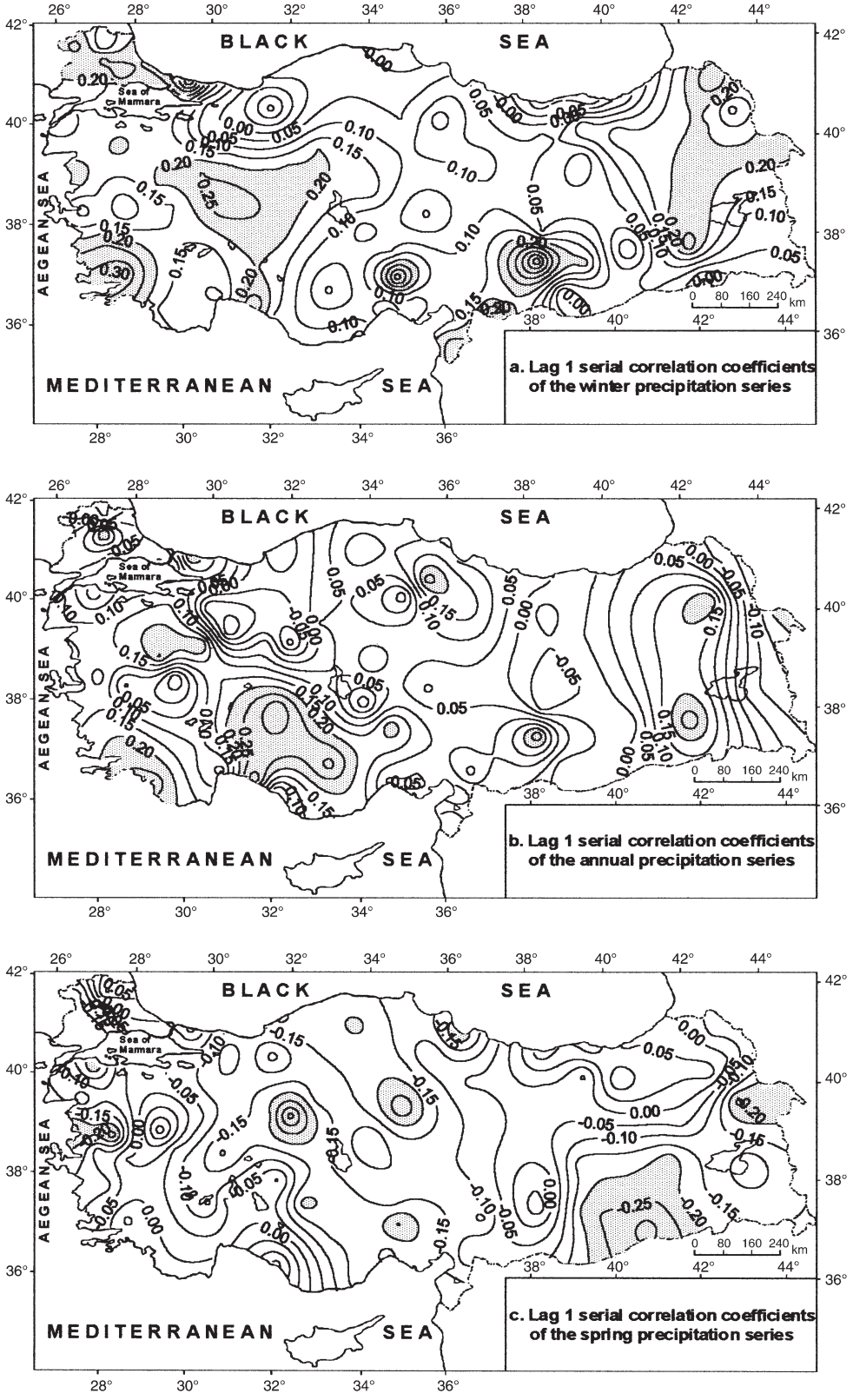

Fig. 2. Spatial distribution patterns of Lag 1 serial correlation coefficients of (a) winter, (b) annual and (c) spring precipitation series of 91 stations. Shaded areas in maps represent significant serial correlation coefficients at the 0.05 significance level

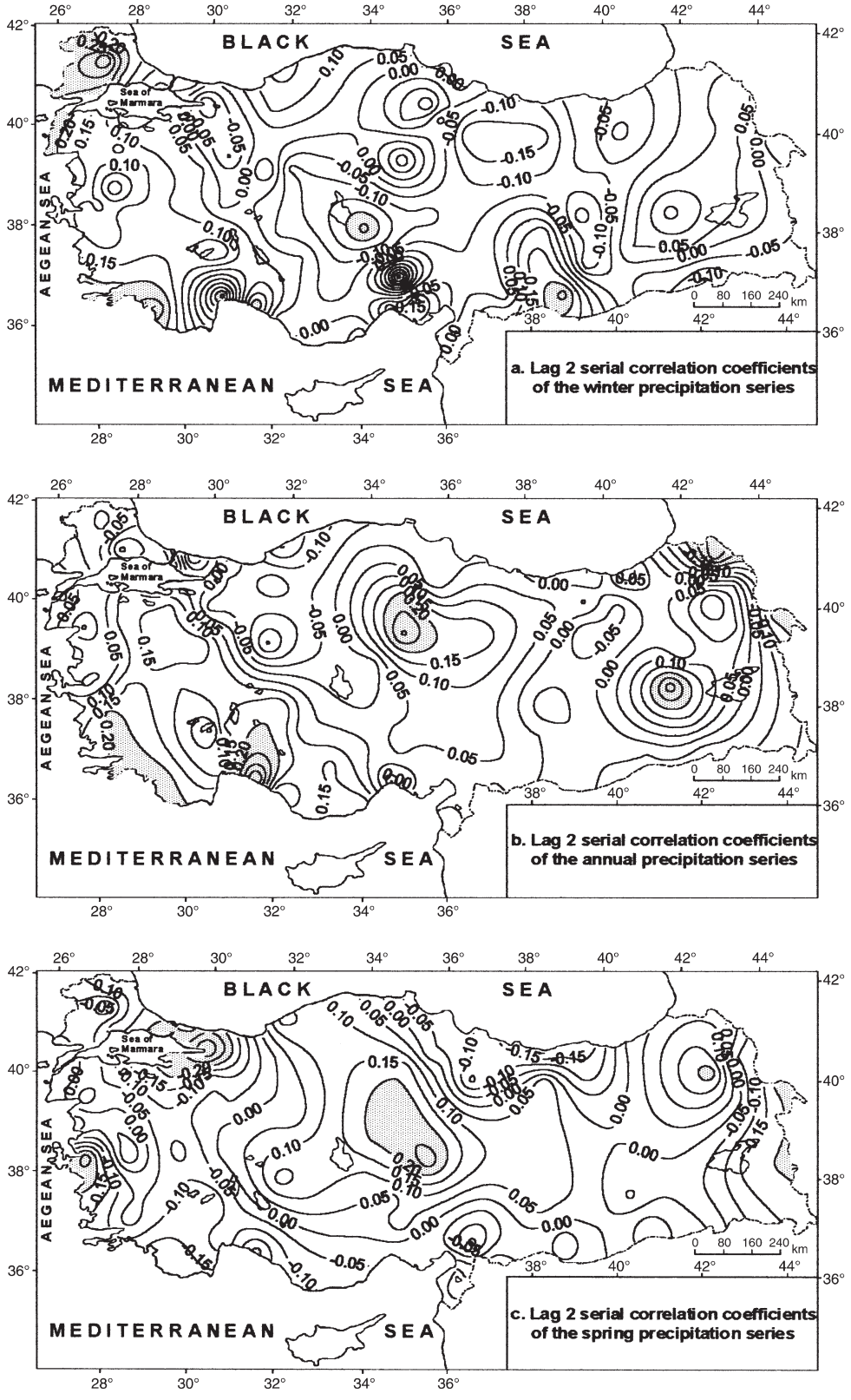

Fig. 3. Spatial distribution patterns of Lag 2 serial correlation coefficients of (a) winter, (b) annual and (c) spring precipitation series of 91 stations. Shaded areas as in Fig. 2

very similar to that in Fig. 2b. The *L*-2*SC* coefficients for the spring precipitation series were found to be highly different compared with those of *L*-1*SC* coefficients for spring. For instance, the spatial distribution pattern of *L*-2*SC* coefficients for spring season (Fig. 3c) shows that positive *L*-2*SC* coefficients take the place of negative *L*-1*SC* coefficients over the CCAN rainfall region. There are 2 coherent regions: the large one characterised by significant positive *L*-2*SC* coefficients over the CCAN rainfall region, and the one with significant negative values over the middle and eastern parts of the MRT region. The coherent region of significant negative *L*-1*SC* coefficients over the CMED rainfall region also disappeared in the distribution pattern of the *L*-2*SC* coefficients for spring precipitation series (Fig. 3c).

Fig. 4 shows the spatial distribution patterns of the Lag 3 serial correlation (*L*-3*SC*) coefficients for winter, annual and spring precipitation series. Some coherent regions with statistically significant values are apparent generally over the western and southern regions, where the Mediterranean type of rainfall regimes are mostly dominant (Fig. 4a,b). Nevertheless, there are some important differences concerning the nature (sign) and spatial distribution pattern of the *L*-3*SC* coefficients in comparison with the *L*-1*SC* coefficients. The main change compared with the *L*-1*SC* coefficients occurs over the CMED and CEAN rainfall regions. For instance, we have a coherent area with significant *L*-3*SC* coefficients and an area of insignificant *L*-3*SC* coefficients over the CMED and CEAN rainfall regions for annual precipitation (Fig. 4b), respectively, whereas a large coherent region with mostly insignificant positive *L*-1*SC* coefficients is evident over a large region over the most eastern region (Fig. 2b).

A simple Markov-type persistence was found in the normalised winter precipitation anomaly series of 11 stations, when a significant positive *L*-1*SC* coefficient and the necessary approximate exponential relationship ($r_2 \cong r_1^2$ and $r_3 \cong r_1^3$) were considered. Some of these stations are located in the colder and more continental northeastern part of the CEAN rainfall region. Significant negative *L*-1*SC* coefficients for the spring precipitation series should be closely related to apparent high-frequency oscillations rather than persistence. Therefore, the white noise continuum was applied to evaluate the basic spectrum computed for the precipitation series of most stations.

4.2. Periodicity

For significance of the spectral estimates, the 0.90 and 0.95 confidence levels of the appropriate null continuum (red or white noise) were taken as a basis for the plots of the power spectrum and for assessing the results. If a time series contains persistence, the spectrum changes over all wavelengths and the amplitude of the spectrum has a decreasing trend from long to short wavelengths. In this case, the spectrum is named red noise. For the spectrum of a precipitation series showing the necessary exponential relationship for simple Markov-type persistence, the appropriate null hypothesis was assumed to be a Markov red noise continuum. A series characterised by an insignificant positive *L*-1*SC* coefficient or a series that has a significant positive *L*-1*SC* coefficient but is not a simple Markov-type, and any series with negative *L*-1*SC* coefficients was evaluated as a white noise continuum. The white noise continuum assumed for the base (theoretical) spectrum of a series is a straight horizontal line; in other words, its value is the same for all wavelengths estimated for the series.

Randomness, persistence and periodic components of series were also examined using correlograms (serial correlation plots). A correlogram is a simple but useful device for determining the degree of dependence existing in successive values of a climatic time-series. It is formed by plotting the *r*-lag (r_L) against the lag (L). In the study, the power spectrum and serial correlation plots of selected stations are given together in order to show the relationship between periodic components and serial correlation coefficients visually. In a pure random series with long-term data, $r_L \cong 0$ for all lags greater than zero (Shaw 1988). However, when especially N is not large, a correlogram is formed by small r_L values mostly varying around zero. If there are several positive serial coefficients among the observation values, the r_1, r_2, r_3, etc., values begin to be reduced after $r_0 = 1$ and finally reach values about zero. They are similar to decreasing the spectral estimates in the series whose power spectrum has Markov-type persistence. This is also an indicator of a Markov process (autoregressive process) (Shaw 1988). The third example is a correlogram of an observational series containing a purely sinusoidal wave that represents a periodic component in the time-series. The cosine curve is repeated for every T time units throughout the correlogram with $r_L = 1$ for $L = 0$, T, $2T$, $3T$, etc. (Shaw 1988). Therefore, the periodicity in time-series appears as regular cycles or waves in the correlogram of that series.

Although time series plots and tables of the results for 91 stations were prepared, only the results of 12 selected stations are given here. To evaluate the power spectrum results, generally period values computed by the equation $P = (2m/L)$ for long-term precipitation series ($N = 62$, 63 and 64 with $m = 21$) were taken into account (Table 2).

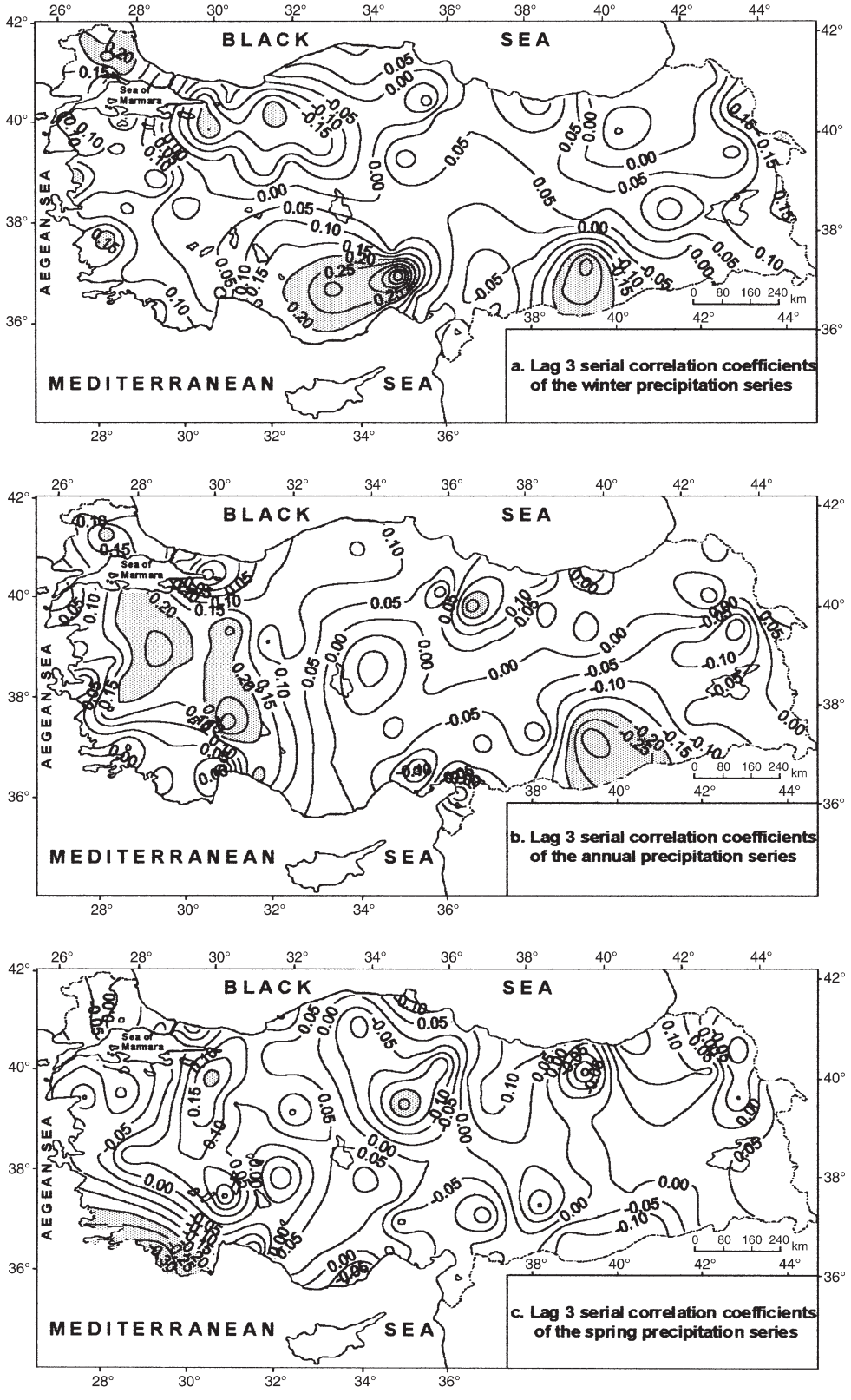

Fig. 4. Spatial distribution patterns of Lag 3 serial correlation coefficients of (a) winter, (b) annual and (c) spring precipitation series of 91 stations. Shaded areas as in Fig. 2

In winter season, long-period fluctuations of 8.4, 12–12.7, 14, 18 and 21 yr are dominant in the MRT and MED rainfall regions, while short-term cycles of 2, 2.1, 3–3.2 yr are evident in the BLS region (Fig. 5, Table 3). Short cycles of 2.8 and 3–3.2 yr were observed at Mersin and Adana in the Eastern Mediterranean subregion. In general, short cycles of 2.2–2.3 yr and 3–3.2 yr and long cycles of 12 yr were dominant in the

Table 2. Periods computed for the long series (N = 62, 63 and 64) and the classification used for their standard assessment. L: lag

L	Period (yr)	Classification	L	Period (yr)	Classification
0	0.0	Non-assessed	11	3.8	Short
1	42.0	Non-assessed	12	3.5	Short
2	21.0	Long	13	3.2	Short
3	14.0	Long	14	3.0	Short
4	10.5	Long	15	2.8	Short
5	8.4	Medium	16	2.6	Short
6	7.0	Medium	17	2.5	Short
7	6.0	Medium	18	2.3	Short – ca. biennial
8	5.3	Medium	19	2.2	Short – ca. biennial
9	4.7	Short	20	2.1	Short – ca. biennial
10	4.2	Short	21	2.0	Short – biennial

Table 3. Results of the serial correlation and power spectrum analyses for the winter precipitation series of 12 selected stations representative of the rainfall regions. L: lag; m: maximum lag; WN: white noise; and RN: red noise

Stn (rainfall region)	Serial correlation coefficient (r_1)	L (m)	Cycle	Chosen continuum
Trabzon (BLS)	−0.164	13 (21)	3.2*	WN
		20 (21)	2.1**	
		21 (21)	2.0**	
Giresun (BLS)	−0.127	13 (21)	3.2*	WN
		14 (21)	3.0**	
İstanbul (MRT)	0.239**	3 (21)	14.0*	RN
Bandırma (MED)	0.190	2 (21)	21.0**	WN
		3 (21)	14.0**	
Muğla (MED)	0.339**	2 (21)	21.0**	WN
		3 (21)	14.0**	
		5 (21)	8.4*	
Mersin (MED)	−0.009	13 (21)	3.2*	WN
		14 (21)	3.0**	
		15 (21)	2.8*	
Elazığ (CMED)	0.041	13 (21)	3.2**	WN
		14(21)	3.0**	WN
Diyarbakır (CMED)	−0.112	13 (21)	3.2*	WN
		17 (21)	2.5*	WN
		18 (21)	2.3**	WN
Siverek (CMED)	0.221**	4 (21)	10.5*	WN
		5 (21)	8.4*	
		6 (21)	7.0**	
		7 (21)	6.0**	
Uşak (MEDT)	0.155	2 (21)	21.0**	WN
Ankara (CCAN)	0.203**	6 (21)	7.0**	WN
		7 (21)	6.0**	
Sarıkamış (CEAN)	0.196**	13 (21)	3.2*	RN
		14 (21)	3.0*	

*Significant for spectral estimates at the 0.90 confidence level;
**Significant for spectral estimates at the 0.95 confidence level; significant for r_1 at the 0.05 significance level

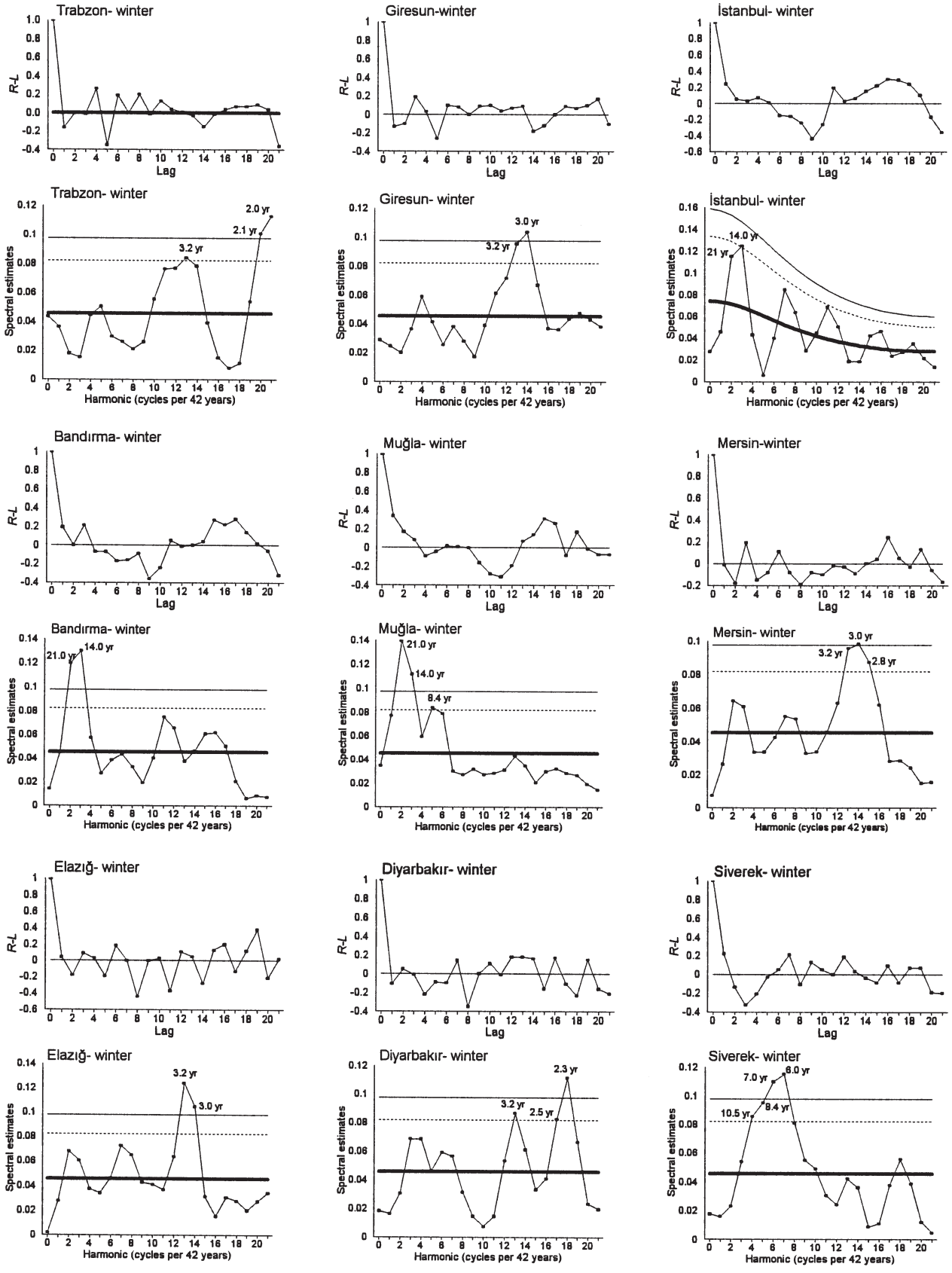

Fig. 5. Correlogram and power spectrum plots for winter precipitation series of 12 selected stations. Power spectra: (—) 'null' ('white' or 'red' noise) continuum; (- - - - -,——) 0.90 and 0.95 confidence limits of the chosen continuum

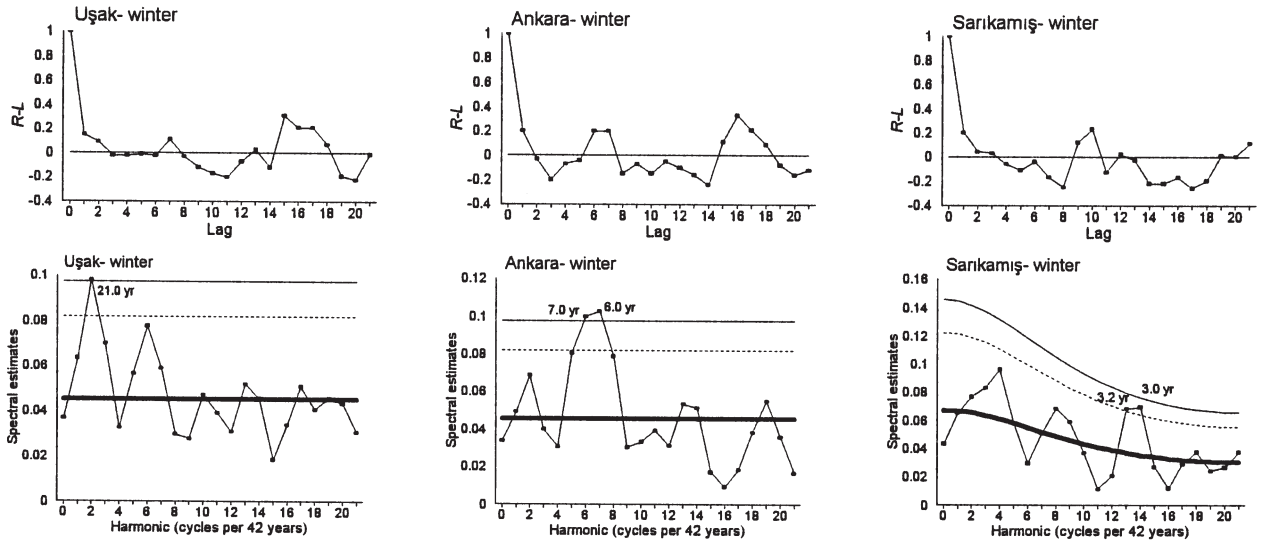

Fig. 5 (continued)

winter precipitation variations of the CMED region. Both long-period fluctuations and short-term oscillations were seen at Adıyaman, Mardin and Gaziantep. The consistent long-period fluctuations of 14 and 21 yr in the MED region are striking. The CCAN region showed generally short-term oscillations of 3–3.2 yr and medium-term fluctuations of 6, 7 and 8.4 yr. The CEAN region was characterised by cycles of about 3–3.2 yr and 7–8 yr.

In the spring season, major peak values dominated over the spectral bands corresponding generally to cycles of 2 yr (2.0, 2.1, 2.3), 3 yr (3.0, 3.2, 3.5), 4 yr (4.0, 4.2, 4.7, 4.8) and 5 yr (5.1, 5.3, 5.4) in most precipitation series (Fig. 6, Table 4). These cycles were characteristic for all the rainfall regime regions.

When the results of all stations were examined together, it was seen that the rainfall variations in the summer season comprised all the periods taken into account in the study (Table 5). Regionally, periodic features in the variations of the summer rainfall series can be summarised as follows:

- short and medium cycles in the BLS rainfall region;
- short cycles of about 3–4 yr and medium cycles of 6 yr in the MRT region;
- short cycles of about 2, 3 and 4 yr at most stations, and long cycles at some stations in the MED region;
- short cycles of about 2 yr and long-term cycles in the CMED region (several stations were random with respect to periodicity);
- short and medium-term cycles in the MEDT region;
- short, medium and long cycles in the CCAN region; and
- short and medium-term cycles of about 2, 3, 4 and 5 yr in the CEAN region.

The autumn precipitation series also included all the periods considered. Regionally, periodicity for the autumn precipitation series is characterised generally by short cycles of 2, 3 and 4 yr in the BLS, MRT and MED rainfall regions (Table 6). The following were also found: short cycles of about 2 yr and long cycles in the CMED region; medium and long cycles in the MEDT region; and short cycles of 2 and 4 yr, medium and long cycles of 8.4, 10.5, 14 and 21 yr in the CCAN region, and biennial cycles in the CEAN region. Autumn precipitation series at some stations in the MEDT and CEAN regions were found to be random with respect to periodicity, and their correlograms and spectral estimates did not contain any marked pattern.

When stations were examined as a whole, the variations of the annual precipitation series was found to contain all the cycles, except cycles of 5.3 and 6 yr (Table 7). Regionally, the periodic component of variations in the annual precipitation series was characterised by following cycles:

- short cycles of 2.5 yr, medium cycles of 8.4 yr and longer cycles in the BLS region;
- short cycles of 3 yr and long cycles of 14, 19 and 21 yr in the MRT region;
- medium cycles of around 7 and 8 yr and long cycles of around 9–10, 12–14, 19–21 yr in the MED region;
- short, medium and long cycles in the CMED region;
- marked long cycles of 14 and 21 yr in the MEDT region;
- short cycles of 2–3 yr, medium cycles of 8.4 yr and long cycles of 10.5, 14 and 21 yr in the CCAN region; and
- short cycles of 3–4 yr and long cycles of 14 and 21 yr in the CEAN region.

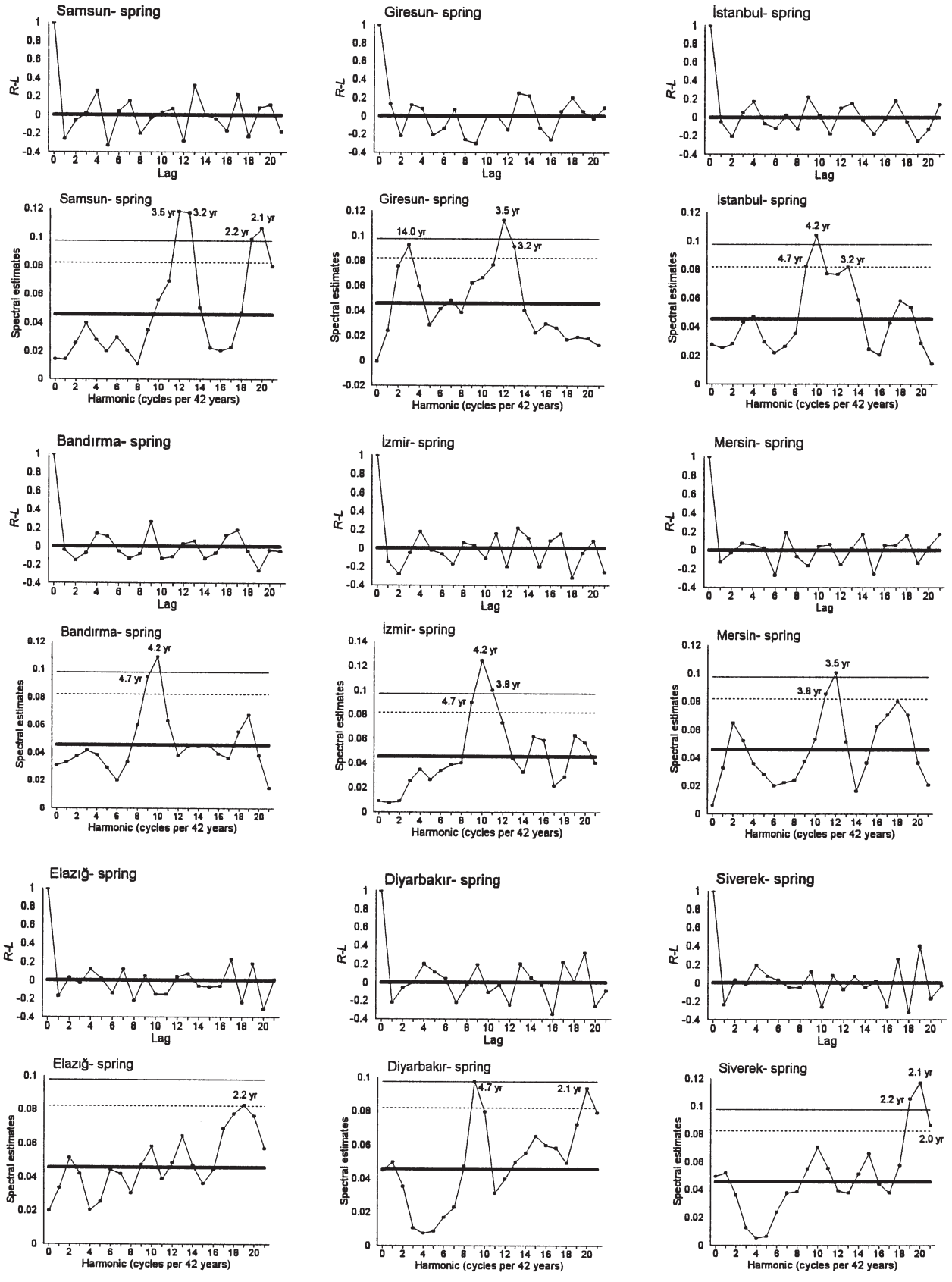

Fig. 6. Correlogram and power spectrum plots for spring precipitation series of 12 selected stations. Lines as in Fig. 5

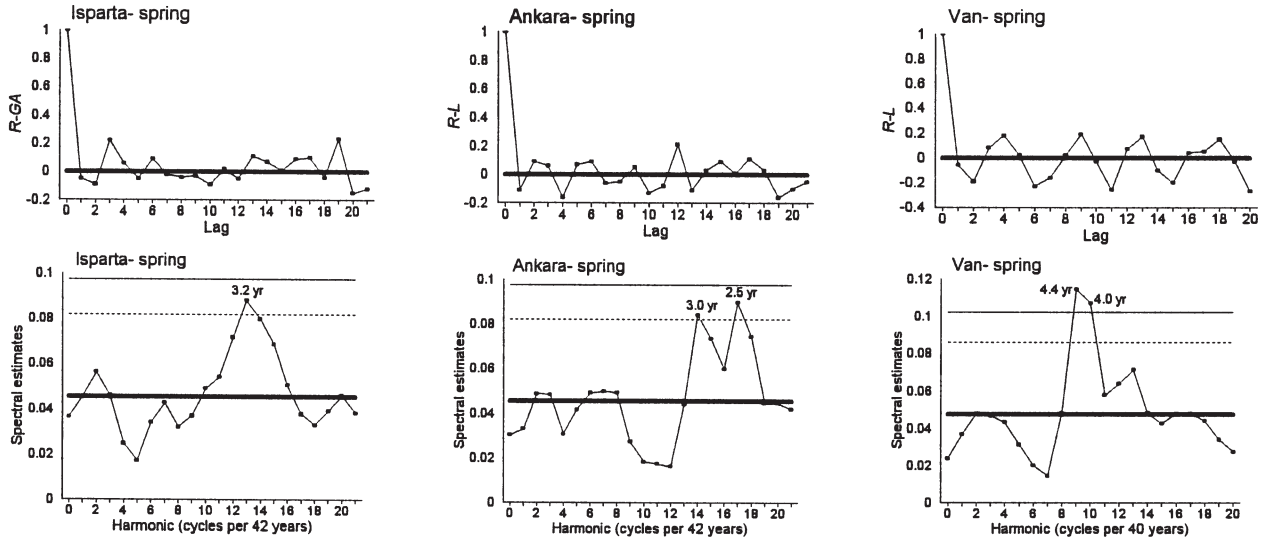

Fig. 6 (continued)

Table 4. Results of the serial correlation and power spectrum analyses for the spring precipitation series of the 12 selected stations. Abbreviations and asterisks as in Table 3

Stn (rainfall region)	Serial correlation coefficient (r_1)	L (m)	Cycle	Chosen continuum
Samsun (BLS)	−0.256**	12 (21)	3.5**	WN
		13 (21)	3.2**	
		19 (21)	2.2**	
		20 (21)	2.1**	
Giresun (BLS)	0.131	3 (21)	14.0*	WN
		12 (21)	3.5**	
		13 (21)	3.2*	
İstanbul (MRT)	−0.050	9 (21)	4.7*	WN
		10 (21)	4.2*	
		13 (21)	3.2*	
Bandırma (MED)	−0.044	9 (21)	4.7*	WN
		10 (21)	4.2**	
İzmir (MED)	−0.151	9 (21)	4.7*	WN
		10 (21)	4.2**	
		11 (21)	3.8**	
Mersin (MED)	−0.129	11 (21)	3.8*	
		12 (21)	3.5**	
Elazığ (CMED)	−0.168	19 (21)	2.2*	WN
Diyarbakır (CMED)	−0.223**	9 (21)	4.7**	WN
		20 (21)	2.1*	
Siverek (CMED)	−0.240**	19 (21)	2.2**	WN
		20 (21)	2.1**	
		21 (21)	2.0*	
Isparta (MEDT)	−0.051	13 (21)	3.2*	WN
Ankara (CCAN)	−0.113	14 (21)	3.0*	WN
		17 (21)	2.5*	
Van (CEAN)	−0.057	9 (20)	4.4**	WN
		10 (20)	4.0**	

Table 5. Results of the serial correlation and power spectrum analyses for the summer precipitation series of the 12 selected stations. Abbreviations and asterisks as in Table 3

Stn (rainfall region)	Serial correlation coefficient (r_1)	L (m)	Cycle	Chosen continuum
Trabzon (BLS)	0.015	9 (21)	4.7**	WN
Giresun (BLS)	0.011	4 (21)	10.5*	WN
		5 (21)	8.4**	
		17 (21)	2.5*	
Bursa (MRT)	0.270**	7 (21)	6.0*	RN
Bandırma (MED)	0.013	10 (21)	4.2*	WN
		11 (21)	3.8**	
		12(21)	3.5**	
		13 (21)	3.2*	
Muğla (MED)	0.021	10 (21)	4.2*	WN
		11 (21)	3.8*	
Mersin (MED)	0.131	2 (21)	21.0*	WN
Kahramanmaraş	0.000	5 (18)	7.2*	WN
(CMED)		16 (18)	2.3*	
		17 (18)	2.1*	
Diyarbakır (CMED)	0.075	4 (21)	10.5*	WN
Siverek (CMED)	0.102	8 (21)	5.3*	WN
		9 (21)	4.7**	
Uşak (MEDT)	−0.090	4 (21)	10.5*	WN
		15 (21)	2.8**	
Ankara (CCAN)	0.166	3 (21)	14.5**	WN
		4 (21)	10.5**	
		5 (21)	8.4**	
Sarykamış (CEAN)	0.053	9 (21)	4.7**	WN
		10 (21)	4.2*	

Table 6. Results of the serial correlation and power spectrum analyses for the autumn precipitation series of the 12 selected stations. Abbreviations and asterisks as in Table 3

Stn (rainfall region)	Serial correlation coefficient (r_1)	L (m)	Cycle	Chosen continuum
Trabzon (BLS)	−0.087	7 (21)	6.0**	WN
		14 (21)	3.0**	
Zonguldak (BLS)	0.065	15 (21)	2.8*	WN
		16(21)	2.6*	
İstanbul (MRT)	−0.127	13 (21)	3.2**	WN
		14 (21)	3.0*	
Balıkesir (MED)	−0.150	14 (19)	2.7**	WN
		15 (19)	2.5**	
Muğla (MED)	0.039	5 (21)	8.4**	WN
		6 (21)	7.0*	
		17 (21)	2.5**	
Mersin (MED)	−0.147	13 (21)	3.2*	WN
		17 (21)	2.5*	
		18 (21)	2.3*	
Malatya (CMED)	0.082	2 (21)	21.0*	WN
Diyarbakır (CMED)	−0.141	18 (21)	2.3*	WN
		19 (21)	2.2**	
		20 (21)	2.1*	
		21 (21)	2.0*	
Şanlıurfa (CMED)	0.015	2 (19)	19.0*	WN
		3 (19)	12.7*	
Isparta (MEDT)	0.166	4 (21)	10.5*	WN
Ankara (CCAN)	−0.157	19 (21)	2.2*	
Sarıkamış (CEAN)	0.150	2 (21)	21.0**	WN
		3 (21)	14.0**	

Table 7. Results of the serial correlation and power spectrum analyses for the annual precipitation series of the 12 selected stations. Abbreviations and asterisks as in Table 3

Stn (rainfall region)	Serial correlation coefficient (r_1)	L (m)	Cycle	Chose continuum
Trabzon (BLS)	−0.006	9 (21)	4.7*	WN
Giresun (BLS)	0.017	5 (21)	8.4*	WN
		17 (21)	2.5*	
İstanbul (MRT)	−0.004	12 (21)	3.5*	WN
		13 (21)	3.2**	
Bandırma (MED)	0.078	2 (21)	21.0*	WN
		3 (21)	14.0**	
		4 (21)	10.5*	
		13 (21)	3.2*	
Muğla (MED)	0.243**	2 (21)	21.0**	WN
		3 (21)	14.0**	
		4 (21)	10.5*	
		5 (21)	8.5**	
		6 (21)	7.0*	
Silifke (MED)	0.172	2 (21)	21.0**	WN
		5 (21)	8.4**	
Kahramanmaraş	0.080	3 (18)	12.0**	WN
(CMED)		4 (18)	9.0*	
		5 (18)	7.2*	
Diyarbakır (CMED)	−0.037	19 (21)	2.2*	WN
		20 (21)	2.1**	
Siverek (CMED)	0.020	19 (21)	2.2*	WN
		20 (21)	2.1*	
Kütahya (MEDT)	0.258**	2 (21)	21.0**	WN
		3 (21)	14.0**	
Eskişehir (CCAN)	−0.187	16 (21)	2.6**	WN
		17 (21)	2.5**	
Sarıkamış (CEAN)	0.253**	2 (21)	21.0**	WN
		3 (21)	14.0**	

4.3. Some relationships with tropospheric variations

A detailed discussion has already been made in Section 1 with regard to the relationships between precipitation variations and various physical mechanisms based on the published literature. In addition, we would like to present an assessment of the relationships between the precipitation anomaly series and the 500 hPa geopotential anomaly series, with respect to both long-term variations and statistical/climatological characteristic of periodicity and persistence. The aim of the discussions in the following sub-sections is to relate variations of the 500 hPa geopotential height anomalies at İstanbul to some of our main findings on the components of periodicity and persistence in the precipitation anomaly series. These would also be helpful to make some physical assessments and/or find explanations for observed temporal and spatial differences in the component of periodicity of precipitation series.

4.3.1. Correlation with 500 hPa geopotential heights

By considering the explanations above, first we examined the nature and magnitude of the relationships between long-term precipitation variations and 500 hPa height variations for annual and seasonal (except summer) normalised anomaly series. The elimination of summer is mainly due to the fact that the summer dryness arising from the large-scale regional climate (i.e. the Mediterranean macro-climate), which is controlled by both mid-latitude and north African-Asiatic tropical (e.g. Monsoon low) pressure systems, influences most of the country, except the Black Sea coastal area and north-eastern Anatolia. The atmospheric control mechanism in summer differs considerably from that in other seasons. Local and/or sub-regional physical geographic factors, such as topography, exposure and continentality, and associated meteorological events (e.g. local convective showers/thunderstorms, orographic rains, etc.) also diminish the

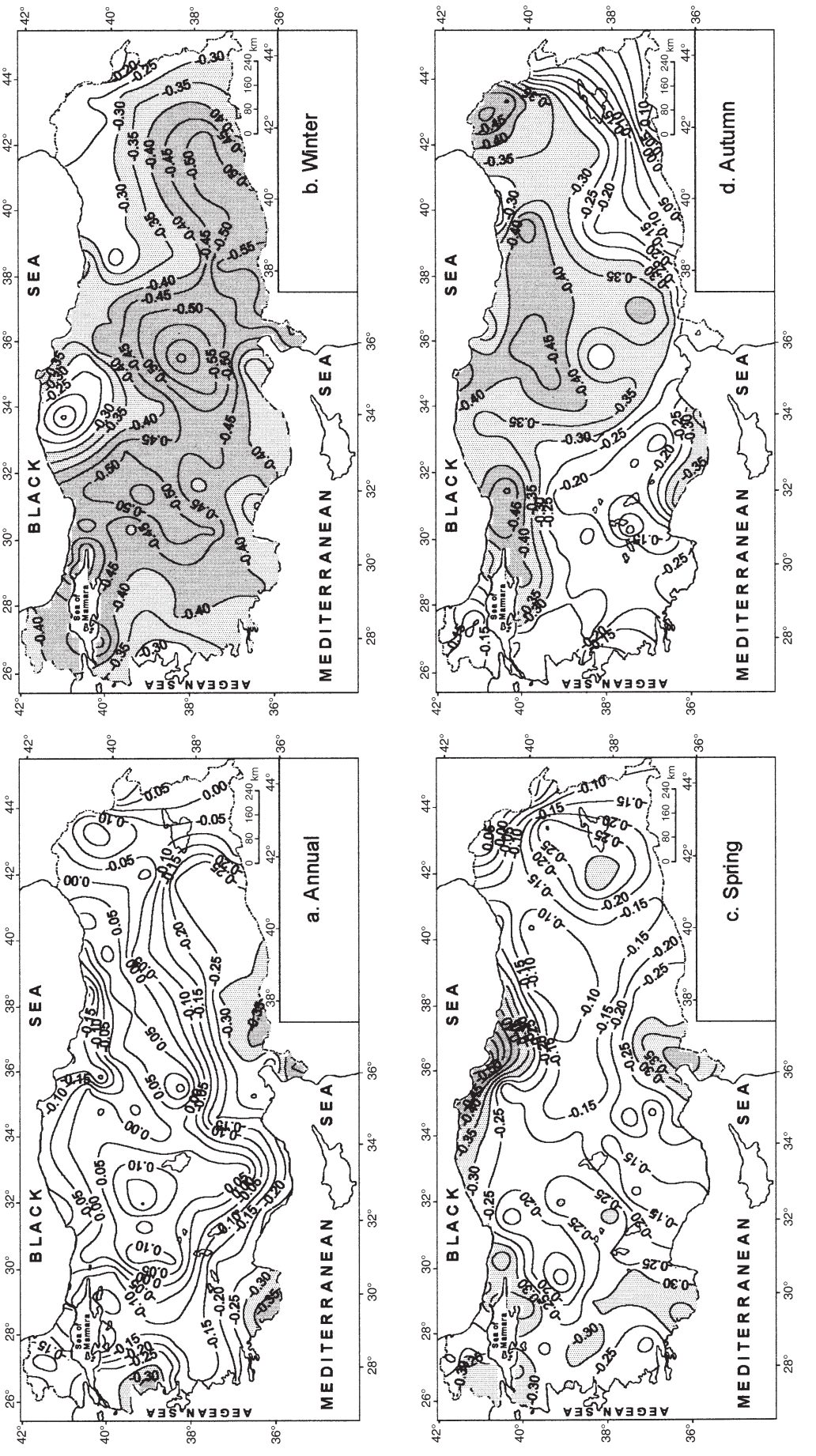

Fig. 7. Spatial distribution patterns of Pearson's *r* correlation coefficients between the normalised 500 hPa geopotential height series of İstanbul and the normalised precipitation series of 91 stations. Light and dark shading represents the areas with correlation coefficients significant at the 0.05 and 0.01 levels, respectively

real effects of regional atmospheric control mechanisms over Turkey in the summer.

A field analysis was made in order to show geographical distribution patterns of the Pearson's correlation coefficient *r* between the precipitation anomalies of 91 stations and the 500 hPa geopotential height anomalies of İstanbul (Fig. 7a–d). In order to perform this spatial analysis, the method of kriging was used to produce contours on spatial distribution maps.

The correlation coefficients show a well-defined but not strong spatial autocorrelation (i.e. geographical relationship) (Fig. 7a). A 2-direction zonality is evident; it is characterised by negative correlation coefficients over the MED and CMED regions, positive and near zero negative correlation coefficients over the continental inner regions and then again negative correlation coefficients over the BLS region. Statistically significant spatial coherence was found over the MED and CMED regions. Inter-annual variations of winter precipitation anomalies were most closely related with variations of 500 hPa geopotential height anomalies (Fig. 7b). Significant negative correlation coefficients of the winter season show a well-defined spatial coherence, except the western and eastern sub-regions of the BLS region, where post-frontal weather processes and orographic rainfall occurrences during the year are dominant, and the northern and far eastern margins of the country. Statistically significant coherent regions at the 0.01 level appear throughout a large zone that extends in the northwest to southeast direction. Spring precipitation anomalies are negatively but not strongly correlated with the 500 hPa geopotential height anomalies. Coherent areas with significant negative correlations cover the MRT, BLS and MED regions and the eastern parts of the CEAN and CMED regions (Fig. 7c). Correlation coefficients are stronger, with a 0.01 significance level, over the middle subregion of the BLS region. The spatial distribution pattern of autumn correlation coefficients is apparently characterised by a 1-direction zonality, with some exceptions found over the MED region (Fig. 7d). Autumn correlation coefficients generally increase from south to north and reach a 0.01 significance level over the western BLS region and northeastern parts of the CCAN and CEAN regions.

Significant negative correlations could be considered as an indicator of the rainfall occurrence areas mainly affected by the atmospheric disturbances (e.g. upper-level lows and troughs). On the other hand, positive and weak negative correlations could be assessed as an indicator of rainfall occurrence in areas where physical geographic factors (e.g. topography, exposure and continentality) are more effective than, or as important as, atmospheric conditions (Türkeş 1998).

4.3.2. Similarity with the periodicity of 500 hPa geopotential heights

As we have already explained in the previous subsection, there are inter-regional differences in periodicity. For instance, we have found long-period fluctuations for the winter precipitation series in the MRT and MED regions, and short-term cycles in the BLS region. There are also inter-seasonal contrasts for the periodicity and persistence characteristics of the precipitation series. For instance, components of year-to-year variability in the winter and spring precipitation series are considerably different from each other at many stations: low-frequency fluctuations are evident in winter, whereas high-frequency oscillations are dominant in the spring. Power spectrum analysis of the 500 hPa geopotential heights at İstanbul was performed for the winter and spring seasons, in order to make some physical explanations for the observed temporal differences between their periodicities.

Inter-annual variation and power spectrum plots of 500 hPa geopotential heights for the winter and spring seasons are given here together with precipitation variations and power spectrum plots of the winter season at İstanbul and the spring season at İstanbul and Ankara (Figs. 8 & 9). This was performed in order to make a visual comparison, or to show the similarity, between atmospheric periodicity and precipitation periodicity. The *L*-1*SC* of the 500 hPa geopotential height anomaly series for winter was found to be positive and significant at the 0.05 level. This significant persistence is very likely related to the observed marked low-frequency fluctuation with an about 13 to 14 yr cycle in the time-series plots (Fig. 8a). The null continuum of the spectrum for the 500 hPa geopotential height and precipitation anomaly series of İstanbul was assumed to be red noise. The prominent spectral peaks with cycles of 2.2–2.3 yr and 14 yr exceed the 0.90 confidence limit for the red noise continuum of the computed spectrum (Fig. 8c). The 14 yr peak also shows up in the spectrum of the winter precipitation anomaly series at İstanbul (Fig. 8d). When the results for all stations are taken into consideration, it appears that for the winter precipitation series the about 12 to 14 yr cycles in the MRT and MED regions and the about 2 yr cycles in the eastern part of the MED region and particularly in the BLS region (Fig. 5, Table 3) are related to the quasi-biennial and 14 yr long periodicity in the winter 500 hPa geopotential height anomaly series at İstanbul. Small differences between the length of cycles of the precipitation and 500 hPa geopotential height series arise from the fact that the length of the 500 hPa geopotential height series is shorter than that of the precipitation series. This situation is also the case for the spring series.

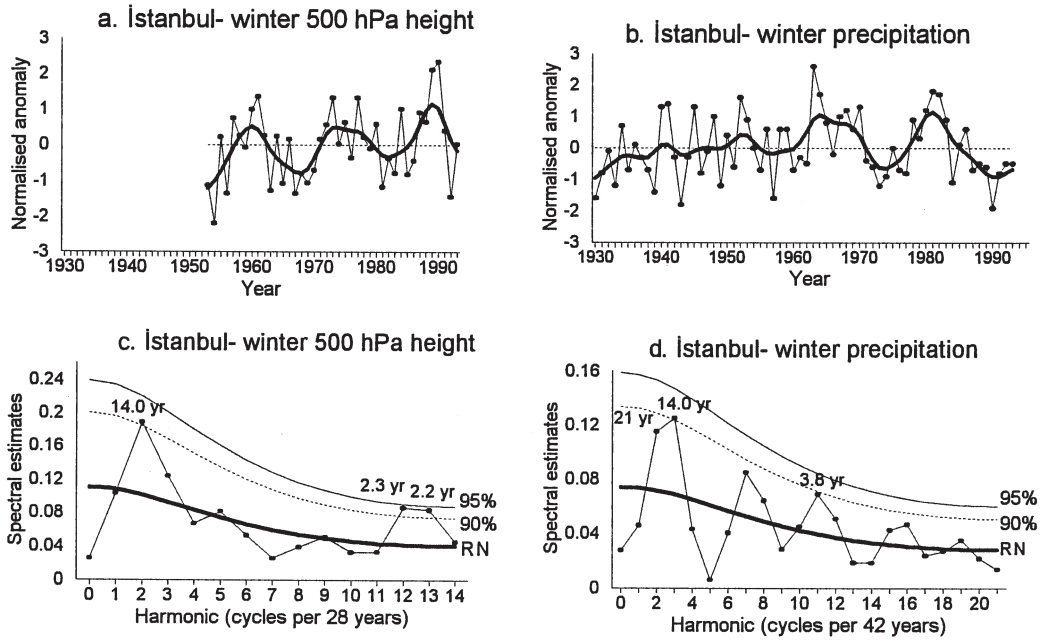

Fig. 8. (a,b) Variations in the normalised winter 500 hPa geopotential height and precipitation series for Istanbul. Inter-annual variations in the series are smoothed by the 9-point Gaussian filter (—) with padded ends. (c,d) Power spectra: (—) 'red noise' (RN) continuum with the 0.90 (- - - - -) and 0.95 (——) confidence limits of the spectrum

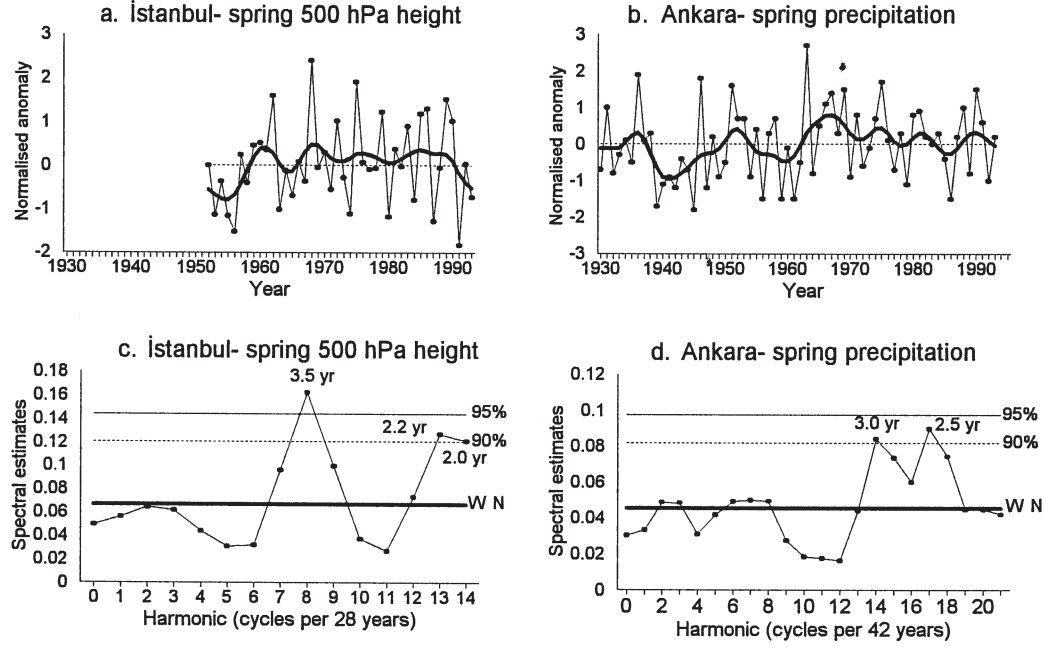

Fig. 9. (a,b) Variations and (c,d) power spectra of the spring 500 hPa geopotential height at İstanbul and the spring precipitation series at Ankara. Line definitions as in Fig. 8

The null continuum of the spectrum for spring 500 hPa geopotential height series is white noise with a negative *L*-1*SC*, as in most spring precipitation series. The white noise continuum of the computed spring spectrum with a negative *L*-1*SC* is a statistical indicator of the observed high year-to-year variability in the time-series plots of variations (Fig. 9a). The spectral peaks with cycles of 2–2.2 yr and 3.5 yr within the spring 500 hPa geopotential height spectrum were significantly different from the 0.90 and 0.95 confidence

limits of the white noise continuum, respectively (Fig. 9c). There was a similarity between the periodicity of the 500 hPa geopotential height and precipitation anomaly series in spring too. The marked oscillations with cycles of 2.5 and 3 yr in the spectrum of the spring precipitation series were significant at the 0.90 confidence level for the Ankara station (Fig. 9b,d). The short-term oscillations with cycles of about 2, 3 and 4 yr were also evident in many spring precipitation series (Fig. 6, Table 4). Thus, the short-cycle oscillations in the spring precipitation series can be explained by the observed high-frequency oscillations of the 500 hPa geopotential heights characterised by the computed cycles of about 2 and 3.5 yr.

5. SUMMARY AND CONCLUSIONS

Serial correlation (autocorrelation) and power spectrum analyses for normalised annual and seasonal precipitation anomaly series of 91 stations and for winter and spring 500 hPa geopotential height anomaly series were carried out in order to detect possible persistence and hidden periodicity in the observed variations of these series. Relationships and similarities between precipitation and 500 hPa geopotential height series were also examined, with respect to long-term variations and statistical/climatological characteristic of periodicity and persistence.

The results of the present study have led to the following main conclusions:

There are considerable inter-regional differences and inter-seasonal contrasts in terms of periodicity and persistence characteristics of precipitation series of Turkey.

L-1*SC* coefficients computed for winter precipitation series are positive at most of the 91 stations, except those in the BLS rainfall region. The persistence in year-to-year variations of winter precipitation series is statistically significant for approximately one-third of the stations. Simple Markov-type persistence was found in the winter precipitation series of 11 stations. Annual precipitation variations of 17 stations revealed a significant positive serial correlation.

Inter-annual variations in the spring precipitation series of most stations, however, have indicated a negative *L*-1*SC* coefficient, 18 of which are statistically significant. Year-to-year variations in some summer rainfall series were explained with positive serial correlation coefficients, whereas variations in some series were dominated by negative *L*-1*SC* coefficients. As for the autumn precipitation series, they have both positive and negative serial correlation coefficients. The autumn series are mostly random with respect to the serial dependence, except at 4 stations.

According to the results summarised above, it should be generally expected that the low-frequency fluctuations and associated long-period cycles exist in winter precipitation series, whereas significant negative *L*-1*SC* coefficients in spring precipitation series should be related closely to the marked high-frequency oscillations rather than persistence.

Winter precipitation series are characterised by long-period fluctuations of 8.4, 12–12.7, 14, 18 and 21 yr in the MRT and MED rainfall regions, whereas cycles of 2, 2.1, 3 and 3.2 yr are evident in the BLS region. Cycles of 2.2–2.3 yr and 3–3.2 yr and cycles of 12 yr are dominant in the CMED region. The CCAN region has short-term oscillations of 3–3.2 yr and medium-term fluctuations of 6, 7 and 8.4 yr. Cycles of about 3–3.2 yr and 7–8 yr were found in the winter precipitation variations of the CEAN region.

Major peak values of most spring precipitation series are dominated generally over the spectral bands with cycles of 2 yr (2.0, 2.1, 2.3), 3 yr (3.0, 3.2, 3.5), 4 yr (4.0, 4.2, 4.7, 4.8) and 5 yr (5.1, 5.3, 5.4).

Variations in the summer rainfall series are characterised by the following cycles: short and medium cycles in the BLS region; cycles of about 3–4 yr and 6 yr in the MRT region; cycles of about 2, 3 and 4 yr at most stations and long cycles at some stations in the MED region; short cycles of around 2 yr and long cycles in the CMED region; and short and medium cycles in the MEDT region. The summer rainfall series exhibit short, medium and long cycles in the CCAN region and cycles of about 2, 3, 4 and 5 yr in the CEAN region.

The periodicity of autumn precipitation series in the BLS, MRT and MED regions was explained by short cycles of around 2, 3 and 4 yr. The following were found: 2 yr cycles (biennial oscillations) and long cycles in the CMED region; medium and long cycles in the MEDT region; cycles of 2, 4, 8.4, 10.5 and 21 yr in the CCAN region; and 2 yr cycles in the CEAN. It is clear that year-to-year variations of spring and autumn precipitation series in most stations exhibit biennial and quasi-biennial periodicity.

There is good consistency between the results of the power spectrum and serial correlation analyses. Precipitation series characterised by a negative serial correlation coefficient or an insignificant positive serial correlation coefficient exhibit short-term oscillations, while precipitation series having a statistically significant positive *L*-1*SC* coefficient at the 0.05 level (or close this level) generally have a periodicity with a long cycle. In the spectrums of precipitation series having a statistically significant negative *L*-1*SC* coefficient, spectral peaks with 2 yr cycles or with cycles slightly longer than 2 yr (quasi-biennial oscillations) are dominant.

Year-to-year variations of winter, spring and autumn precipitation series are closely associated with variations of the 500 hPa geopotential height series at the İstanbul radiosonde station. In winter, negative correlation coefficients (Pearson's *r*) that are statistically significant at the 0.01 level exhibit an apparent spatial coherence over most of Turkey. Spring precipitation series are also negatively correlated with the 500 hPa geopotential height series. Coherent areas with significant negative correlation coefficients exist over the MRT, BLS and MED regions and the eastern parts of the CEAN and CMED regions. In autumn, the geographical distribution pattern of the significant negative correlation coefficients show an apparent spatial coherence over much of Turkey, except the mid- and southwestern and southeastern regions. Coherent areas with statistically significant correlation coefficients at the 0.01 level cover the western BLS and northeastern parts of the CCAN and CEAN regions.

In the upper atmospheric pressure level conditions of Turkey, low-frequency fluctuations in winter and high-frequency oscillations in spring are evident. The prominent spectral peaks with the cycles of 2.2–2.3 yr and 14 yr exceed the 0.90 confidence limit of the red noise continuum for the spectrum of winter 500 hPa geopotential height anomaly series at İstanbul. For winter precipitation series, about 12 to 14 yr long cycles in the MRT and MED regions, and about 2 yr cycles in the eastern part of the MED region and particularly in the BLS region are related to the quasi-biennial and 14 yr long periodicity in the winter 500 hPa geopotential height series. The spectral peaks with the cycles of 2–2.2 yr and 3.5 yr in spring 500 hPa geopotential height spectra are statistically significant at the 0.90 and 0.95 confidence limits of the white noise continuum, respectively.

Similarity was found between the periodicity of the 500 hPa geopotential height and precipitation anomaly series in spring too. The short-term oscillations with cycles of about 2, 3 and 4 yr are evident in many spring precipitation series. Thus, the causes of the biennial and quasi-biennial oscillations in spring precipitation series are the observed high-frequency oscillations of 500 hPa geopotential heights characterised by the computed cycles of about 2 and 3.5 yr.

High-frequency oscillations with short-cycle periodicity dominant in the upper atmospheric level conditions are reflected in the spring precipitation series, although local atmospheric processes begin to be active with respect to precipitation occurrence in spring. This is also true with respect to the weather conditions in the spring season, because weather is highly variable in spring, as we know from synoptic weather types and daily life.

In addition to the main findings listed above, it was also previously shown by Türkeş (1998) that Turkish precipitation is generally related to the location, fluctuation and activity of pressure centres. Consequently, our results particularly for winter, spring and autumn seasons are significant and verifiable with respect to the atmospheric variations and atmospheric control mechanisms.

Finally, we would like to recommend that the dominant persistence and periodicity features of winter, spring and autumn precipitation series revealed by this study be taken into account in seasonal precipitation predictions and model studies, every kind of climate planning and water resources management activities including drought management.

Acknowledgements. The authors wish to thank 2 anonymous reviewers for their valuable comments and constructive recommendations.

LITERATURE CITED

Anyadike RNC (1993) Seasonal and annual rainfall variations over Nigeria. Int J Climatol 13:567–580

Bardossy A, Muster H (1993) Comparison of interpolation methods of daily rainfall amounts under different meteorological conditions. Report of a GEWEX workshop on analysis methods of precipitation on a global scale, WCRP-No. 81, WMO-TD No. 588, Koblenz

Blackman RB, Tukey JW (1958) The measurement of power spectra. Dover Publications, New York

Cressie NAC (1991) Statistics for spatial data. John Wiley, New York

Delfiner P, Delhomme JP (1975) Optimum interpolation by kriging. In: Davis JC, McCullagh MJ (eds) Display and analysis of spatial data. John Wiley, New York, p 96–119

Drosdowsky W (1993) An analysis of Australian seasonal rainfall anomalies: 1950–1987. II: Temporal variability and teleconnection patterns. Int J Climatol 13:111–149

Granger OE (1977) Secular fluctuations of seasonal precipitation in lowland California. Mon Weather Rev 105:386–397

Jenkins GM, Watts DG (1968) Spectral analysis and its applications. Holden-Day, San Francisco

Julian PR (1967) Variance spectrum analysis. Water Resour Res 3:831–845

Kozuchowski KM (1993) Variations of hemispheric zonal index since 1899 and its relationships with air temperature. Int J Climatol 13:853–864

Kutiel H, Hirsch-Eshkol TR, Türkes M (2001) Sea level pressure patterns associated with dry or wet monthly rainfall conditions in Turkey. Theor Appl Climatol 69:39–67

Mächel H, Kapala A, Flohn H (1998) Behaviour of the centres of action above the Atlantic since 1881. Part I: characteristics of seasonal and interannual variability. Int J Climatol 18:1–22

Maheras P, Xoplaki E, Kutiel H (1999) Wet and dry monthly anomalies across the Mediterranean basin and their relationship with circulation, 1860–1990. Theor Appl Climatol 64:189–199

Matalas NC (1967) Time series analysis. Water Resour Res 3: 817–829

Nicholson SE, Palao IM (1993) A re-evaluation of rainfall vari-

ability in the Sahel. Part I. Characteristics of rainfall fluctuations. Int J Climatol 13:371–389
Ogallo L (1979) Rainfall variability in Africa. Mon Weather Rev 107:1133–1139
Rodhe H, Virji H (1976) Trends and periodicities in East African rainfall data. Mon Weather Rev 104:307–315
Shaw EM (1988) Hydrology in practice. VNR International, London
Tukey JW (1950) The sampling theory of power spectrum estimates. In: Symposium on applications of autocorrelation analysis to physical problems. US Office of Naval Research, NAVEXOS-P-735, Washington, DC, p 47–67
Türkeş M (1995) Trends and fluctuations of annual and seasonal rainfall data in Turkey. Türkiye Ulusal Jeodezi-Jeofizik Birliği (TUJJB) Bilimsel Kongresi Bildiriler Kitabı, Harita Genel Komutanlığı, Ankara, p 694–706 (in Turkish)
Türkeş M (1996) Spatial and temporal analysis of annual rainfall variations in Turkey. Int J Climatol 16:1057–1076
Türkeş M (1998) Influence of geopotential heights, cyclone frequency and Southern Oscillation on rainfall variations in Turkey. Int J Climatol 18:649–680
Türkeş M (1999) Vulnerability of Turkey to desertification with respect to precipitation and aridity conditions. Tr J Eng Environ Sci 23:363–380
Türkeş M (2002) Spatial and temporal variations in precipitation and aridity index series of Turkey. In: Bolle HJ (ed) The Mediterranean climate: variability and trends. Proc RICAMARE workshop on the assessment, assimilation and validation of data for 'Global Change' related research in the Mediterranean area, Casablanca, 21–24 February 2001. Springer Verlag, Heidelberg (in press)
Wiener N (1930) Generalized harmonic analysis. Acto Math 55:117–258
Wiener N (1949) Extrapolation, interpolation, and smoothing of stationary time series. Wiley and Technology Press, Cambridge, MA
WMO (1966) Climatic change. WMO Technical Note 79, World Meteorological Organization, Geneva
Xoplaki E, Luterbacher J, Burkard R, Patrikas I, Maheras P (2000) Connecting between the large-scale 500 hPa geopotential height fields and precipitation over Greece during wintertime. Clim Res 14:129–146

Editorial responsibility: Laurence Kalkstein, Newark, Delaware, USA

Submitted: August 15, 2000; Accepted: October 2, 2001
Proofs received from author(s): May 18, 2002